



HAL
open science

S-glycosyltransferase UGT74B1 can glycosylate both S- and O-acceptors: mechanistic insights through substrate specificity

P. Lafite, Sami Marroun, Gaël Coadou, S. Montaut, S. Marques, M. Schuler,
P. Rollin, A. Tatibouët, R. Daniellou, Hassan Oulyadi

► To cite this version:

P. Lafite, Sami Marroun, Gaël Coadou, S. Montaut, S. Marques, et al.. S-glycosyltransferase UGT74B1 can glycosylate both S- and O-acceptors: mechanistic insights through substrate specificity. *Molecular Catalysis*, 2019, 479, pp.110631. 10.1016/j.mcat.2019.110631 . hal-02330966

HAL Id: hal-02330966

<https://normandie-univ.hal.science/hal-02330966v1>

Submitted on 20 Jul 2022

HAL is a multi-disciplinary open access archive for the deposit and dissemination of scientific research documents, whether they are published or not. The documents may come from teaching and research institutions in France or abroad, or from public or private research centers.

L'archive ouverte pluridisciplinaire **HAL**, est destinée au dépôt et à la diffusion de documents scientifiques de niveau recherche, publiés ou non, émanant des établissements d'enseignement et de recherche français ou étrangers, des laboratoires publics ou privés.

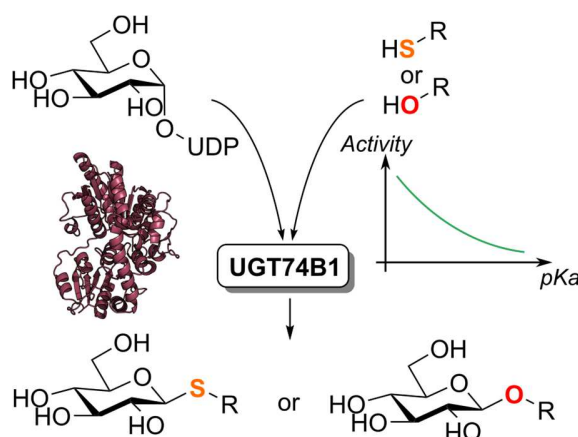


Distributed under a Creative Commons Attribution - NonCommercial 4.0 International License

Abstract

UGT74B1 from *Arabidopsis thaliana* is one of the few characterized glycosyltransferases able to generate a thioglycosidic linkage *in vivo*, using the sulfur atom of thiohydroximate as the nucleophile in the glycosylation reaction. This critical biosynthetic step in glucosinolate production has been documented. Yet little is known about the molecular mechanism that enables this rare and unusual glycosylation at the sulfur atom. To identify the role of this atom in the glycosylation reaction and unraveling the mechanism of UGT74B1, we used a range of substrates containing either sulfur or oxygen. We first demonstrated that the enzyme could catalyze the glycosylation of thiohydroximates but also of *O*-containing hydroximate analogs. If K_M values were shown to be close between analogs, the reaction catalytic rate k_{cat} was 50-100 lower in the case of hydroximates. The glycosylation reaction is catalyzed through deprotonation of the acceptor, which was confirmed by the removal of catalytic carboxylic residues by site-directed mutagenesis. Moreover, using a range of simple phenols and thiophenols as UGT74B1 substrate acceptors for glycosylation, we concluded that the glycosylation reaction rate is correlated to the acceptor atom acidity, and not to the nature of this nucleophilic atom (oxygen or sulfur).

Graphical Abstract



Keywords

Glucosyltransferase, glycosylation, enzyme mechanism, sulfur, *Arabidopsis thaliana*

Abbreviations

GT, Glycosyltransferase; PATH: Phenylacetothiohydroximate; PPTH: Phenylpropanothiohydroximate; PAH: Phenylacetohydroximate; PPH: Phenylpropanohydroximate; CTP: Chlorothiophenol; TP: Thiophenol; TCP: Trichlorophenol; DCP: Dichlorophenol; CP: Chlorophenol.

1 **1. Introduction**

2 Glycosyltransferases (GT) (EC: 2.4.x.x) catalyze the transfer of a sugar from an activated donor to an
3 acceptor [1]. Nucleotide-sugar utilizing GTs, known as Leloir enzymes, are the most abundant group, and
4 the molecular mechanisms that lead to the formation of the glycosidic [2] bond have been widely studied,
5 for retaining or inverting GTs, considering the stereochemistry of the anomeric carbon of the glycoside [3].
6 In the case of inverting GTs, a SN₂ reaction takes place, involving a single displacement step with the
7 formation of an oxocarbenium ion-like transition state. Moreover, a catalytic base residue located in the
8 active site can generally increase the nucleophilicity of the acceptor-attacking atom to generate the
9 glycosidic linkage.

10 Whereas the canonical *O*- and *N*-glycoconjugates are involved in a wide range of biological processes,
11 [4,5] the more unusual *S*- or *C*-glycosides also exhibit many biological roles, for instance in protein
12 glycosylation [6]. Moreover, the nature of the atom in the glycosidic linkage can influence the chemical and
13 physical properties of the glycoconjugates. Especially, *S*-glycosides are of particular interest because they
14 are structural analogs of their *O*-counterparts, while being much more resistant to chemical and/or enzymatic
15 hydrolysis [7–10]. However, though GT engineering has been extensively investigated to increase substrate
16 promiscuity and specificity towards sulfur containing acceptors [11–14], little is known still about the
17 influence of the nucleophilic atom on substrate specificity. Even though several examples of GTs exhibiting
18 dual or triple activity with either *O*-, *S*-, *N*-, or *C*-containing acceptors have been reported [15–22], the
19 molecular mechanism underlying this promiscuity was never discussed. However, Gutmann *et al.* have
20 managed to identify active site motifs that could turn an *O*-GT into a *C*-GT [23,24].

21 In this context, we have recently reported the UDP-sugar donor specificity of UGT74B1, making this
22 versatile GT a strong candidate for biosynthesis of *S*-glycoconjugates [25]. Along with ThuS and SunS,
23 involved in *S*-glycosylation of bacteriocin peptides [26–29], UGT74B1 from *Arabidopsis thaliana* is one
24 of the only *S*-GTs involved in the natural biosynthesis of the most historically known *S*-glycosides, namely
25 glucosinolates [30,31]. Herein, we have studied UGT74B1 and identified the mechanism that leads to its
26 specificity for *S*-glycosylation *versus* *O*-glycosylation, using a diverse panel of acceptor substrates.

27 **2. Materials and methods**

28 **2.1 Chemicals**

29 All used chemicals and buffers were of the highest purity available. HPLC solvents, phenols,
30 thiophenols, pyruvate kinase, lactate dehydrogenase, phosphoenolpyruvate, NADH were purchased from
31 Sigma-Aldrich (Merck). Molecular biology and microbiology chemicals were purchased from
32 ThermoFisher. UDP- α -D-glucose was obtained from Carbosynth Ltd (UK).

33

1 ¹H NMR and ¹³C NMR spectra of synthesized compounds were recorded on Bruker Avance II 400 or Bruker
2 DPX 250 spectrometers. Assignments are based on DEPT 135 sequence and on homo- and heteronuclear
3 correlations. Chemical shifts are reported in parts per million (ppm) from tetramethylsilane as the internal
4 standard. Coupling constants (J) are reported and expressed in Hertz (Hz); splitting patterns are designed
5 as br (broad), s (singlet), d (doublet), dt (doublet of triplets), t (triplet) and m (multiplet). High-resolution
6 mass spectra (HRMS) were obtained with a Maxis Bruker 4G instrument from the “Fédération de
7 Recherche” ICOA/CBM (FR2708) platform in the electrospray ionization (ESI) mode. Infrared spectra of
8 compounds were recorded with a Thermo Scientific Nicolet iS10 spectroscope.

9 Preparation of PAH and PPH was adapted from published literature [32]. 1,1'-Carbonyldiimidazole (1.2
10 equiv.) was added to phenylpropanoic acid or phenylacetic acid (6 mmol, 1 equiv.) dissolved in CH₃CN (20
11 mL) under argon atmosphere and the mixture was stirred at 22 °C for 1h. A solution of NH₂OH (50 wt. %
12 in H₂O, 2 ml, 5 equiv.) was then added and the reaction mixture was stirred at 22 °C for 20h. After
13 concentration under reduced pressure, H₂O (15 mL) was added to the residue and the aqueous solution was
14 extracted with EtOAc (3 x 15 mL). The combined organic phase was washed with brine (1 x 25 mL), dried
15 over Na₂SO₄, filtered and evaporated under reduced pressure. The residue was purified by Reveleris®
16 column chromatography on C18 silica gel (H₂O 100% to CH₃CN 100%) to afford the desired products as a
17 slightly greenish powders.

18 PAH (Figure S1): 682 mg, 75% yield. ¹H NMR (250 MHz, DMSO-d₆): δ 10.59 (s, 1H, OH), 8.77 (s, 1H,
19 NH), 7.28-7.14 (m, 5H, H-Ar), 3.26 (s, 2H, CH₂).[33,34]

20 PPH (Figure S2): 761 mg, 65% yield. ¹H NMR (400 MHz, DMSO-d₆): δ 10.36 (s, 1H, OH), 8.70 (s, 1H,
21 NH), 7.27-7.17 (m, 5H, H-Ar), 2.80 (t, 2H, J = 7.7 Hz, H-3), 2.25 (t, 2H, J = 7.7 Hz, H-2). [33,34].

22

23 **2.2 1.2 Cloning and expression of UGT74B1.**

24 UGT74B1 was cloned as a histidine-tagged protein in *E. coli* and purified as previously reported [25].
25 Site-directed mutagenesis were carried out using QuikChange II XL Site-Directed Mutagenesis kit (Agilent)
26 using WT-UGT74B1 plasmid as DNA template. Primers used for site-directed mutagenesis are presented
27 in Table S1 in Supplementary data. Mutagenesis products were directly transformed into XL10-Gold
28 ultracompetent cells (Agilent) by heat shock method. Each mutant sequence DNA was sequenced (Eurofins
29 genomics) and confirmed to be identical to the known wild-type enzyme sequence DNA except the targeted
30 codon (either His22 and Asp113) replaced by alanine.

31

32 **2.3 Enzymatic assay (Enzyme-coupled)**

33 Determination of enzymatic glycosylation for thiohydroximates PATH, PPTH and hydroximates PAH,
34 PPH were done using a tri-enzymatic assay that couples UDP formation with NADH consumption, using

1 pyruvate kinase and lactate dehydrogenase as enzymatic mixture. Reactions conditions were identical to
2 those reported previously [25]. Kinetics data were analyzed and fitted using Prism 4 (GraphPad).

3 4 **2.4 Enzymatic assay (HPLC separation)**

5 For thiophenols and phenols, an HPLC separation methodology was used to quantify enzymatic activity.
6 A reaction (200 μ L total volume) containing 1mM UDP-glucose, acceptor (20 μ L in 100% MeOH – final
7 concentrations ranging from 50 to 5000 μ M) in 20 mM Tris buffer pH 8.0 was started by addition of 1 μ M
8 UGT74B1. The reaction was left for 15 min at 37°C, then 200 μ L of quenching reagent (CH₃CN:HCOOH,
9 10:1) was added to the mixture. Proteins were precipitated by centrifugation for 10 min at 10,000 rpm, and
10 the supernatant was analyzed by reverse-phase HPLC on a Zorbax Eclipse XDB-C18 column 4.6 \times 150 mm
11 (Agilent) on an Agilent 1220 Infinity II LC System. The mobile phase was delivered at a rate of 1 mL/min
12 with a gradient from A (0.1% HCOOH in H₂O) to B (0.1% HCOOH in CH₃CN) (10% B for 4 min, 10% to
13 60% B in 10 min, 60% to 100% B in 2 min.). The column effluent was monitored at 250 nm.

14 15 **2.5 NMR structural study of desulfo-glucotropaelin**

16 NMR spectra of glucosylated PATH product were recorded in DMSO-*d*₆ solution at 313K on a Bruker
17 AVIII 500 spectrometer operating at 500.13 MHz for ¹H and 125.13 MHz for ¹³C. 1D and 2D experiments
18 (1D ¹H, 2D ¹H-¹H COSY, ¹H-¹H NOESY, ¹H-¹³C HMQC and HMBC) were run under TopSpin (version
19 3.2, Bruker Biospin, Karlsruhe) with a BBFO {¹H, X} probe and a z gradient coil giving a maximum
20 gradient of 50 G cm⁻¹. ¹H and ¹³C chemical shifts were referenced to the solvent residual signals of DMSO-
21 *d*₆ (δ 2.49 for ¹H and 39.70 ppm for ¹³C).

22 23 **2.6 Saturation transfer difference**

24 STD spectra of the mixture of UGT74B1 (100 μ M) with UDPG (1 mM) in phosphate buffer pH=7.3 were
25 undertaken on a Bruker Avance III 600 equipped with CPTXI-cryoprobe. The experiments were acquired
26 with the standard Bruker stddiffesgp.3 sequence by using trains of E-Burp-1 90° selective pulses. Selective
27 pulses were applied at 0 ppm for the on resonance STD excitation, and -17.00 ppm for the difference
28 spectrum, with respect to H₂O at 4.70 ppm. The spectra were measured with 8080 scans after eight dummy
29 scans and lasted approximately 39 hours.

30 31 **2.7 pKa determination by NMR**

32 Thiohydroxamic and hydroxamic acids, and CTP were first characterized by NMR on a Bruker Avance III
33 600 equipped with a CPTXI-cryoprobe. Then, ¹H chemical shifts of these compounds were monitored for
34 pH in order to determine their pKa in a 90:10 mixture of phosphate buffer pH 7.3 and methanol (CD₃OH).
35 The method consists of making 1D ¹H acquisitions following successive additions of acid or base. Labile

1 protons are not detectable under these experimental conditions (phosphate buffer) because they undergo
2 rapid exchange. The chemical shift of the H α protons closest to the deprotonation site is the one which is
3 followed by this method. A titration curve was established by following the chemical shift of the chosen
4 proton as a function of the pH. The obtained data were fitted with an asymmetrical sigmoidal function,
5 which gave the value of the pKa.

6 7 **2.8 pKa calculations**

8 Phenols and thiophenols pKa were calculated using ACD/Labs software.

9 **3. Results**

10 **3.1 UGT74B1 is able to glycosylate O-acceptors**

11 Phenylacetothiohydroximate (PATH) and phenylpropanothiohydroximate (PPTH) (Fig. 1.A) were
12 previously reported to undergo efficient S-glycosylation, with second order catalytic rate k_{cat}/K_M above 10^5
13 $\text{min}^{-1}.\text{mM}^{-1}$ (Table 1) [25]. The O-containing analogues of PATH and PPTH, respectively
14 phenylacetohydroximate (PAH) and phenylpropanohydroximate (PPH) were synthesized using slightly
15 modified reported methods [32]. Both hydroximates were used in UGT74B1 glycosylation assays following
16 the same procedure, and their catalytic constants were determined (Table 1). Both O-acceptors have μM
17 range K_M similar to those calculated for thiohydroximates PATH and PPTH. However, the catalytic turnover
18 is dramatically decreased when swapping the sulfur atom for the oxygen atom, as k_{cat} of a hydroximate is
19 100-fold lower than the one for the corresponding thiohydroximate. UGT74B1 can thus bind hydroximates
20 as efficiently as thiohydroximates, as K_M values lie in the same order of magnitude. However, the reactivity
21 of the oxygen atom in hydroximates is much lower than that of sulfur atom in PATH and PPTH, yielding
22 lower catalytic rate k_{cat} and catalytic efficiency k_{cat}/K_M .

23
24

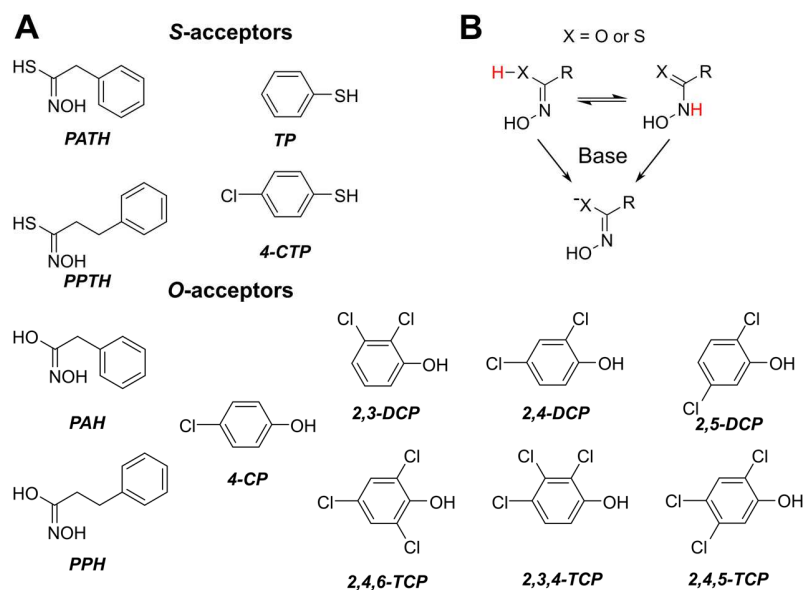


Figure 1: (A) UGT74B1 substrates used in this study. (B) Tautomeric equilibrium and deprotonation of thiohydroximates and hydroximates.

<i>UGT74B1</i> variant	Acceptor	K_M (μM)	k_{cat} (min^{-1})	k_{cat}/K_M ($\text{min}^{-1}\cdot\text{mM}^{-1}$)
Wild-type	PATH ^a	3.1 ± 0.6	280 ± 58	90×10^3
	PPTH ^a	2.2 ± 0.5	326 ± 95	148×10^3
	PAH	1.1 ± 0.2	3.9 ± 1.3	3.5×10^3
	PPH	0.9 ± 0.2	4.3 ± 1.2	4.8×10^3
<i>His22Ala</i>	PATH	<i>n.d.</i> ^b	<i>n.d.</i>	<i>n.d.</i>
	PPTH	<i>n.d.</i> ^b	<i>n.d.</i>	<i>n.d.</i>
<i>Asp113Ala</i>	PATH	27.2 ± 4.5	1.2 ± 0.1 ^c	
	PPTH	58.9 ± 11.4	2.4 ± 0.1 ^c	

Table 1: Catalytic constants of UGT74B1 (wild-type and mutated) towards thiohydroxamic and hydroxamic acids. Values were obtained at 37°C, pH 8.0. *PATH* : Phenylacetothiohydroximate ; *PPTH* : Phenylpropanothiohydroximate ; *PAH* : Phenylacetohydroximate ; *PPH* : Phenylpropanohydroximate.^a

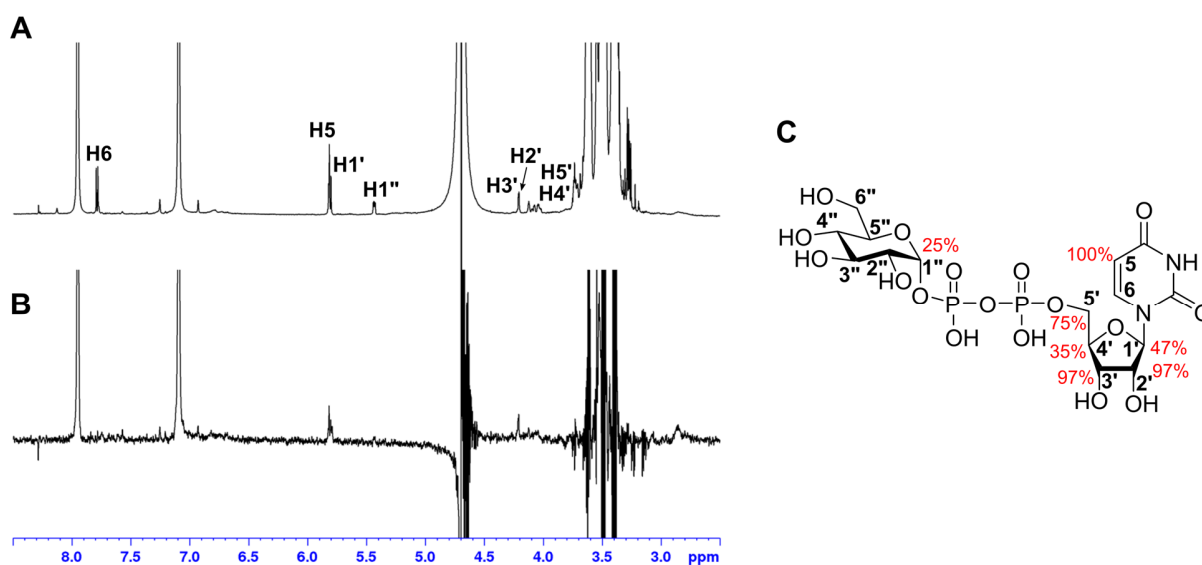
From reference 31. ^b*n.d.* non detectable. ^c: V_{max} in $\mu\text{M}\cdot\text{min}^{-1}$

3.2 UGT74B1 requires an acidic acceptor

UGT74B1 belongs to the CAZy GT1 family [35], and we have previously built an homology model using several GT1 templates, and identified residues surrounding the active site [25]. A NMR structural

1 study of glucosylated PATH (namely desulfo-glucotropaelin [25,36]) product solution was undertaken in
 2 DMSO-*d*₆ (Fig S3-S7). This allowed for a complete assignment of protons signals for desulfo-
 3 glucotropaelin, showing reverse anomeric carbon stereochemistry between UDP- α -D-glucose donor and
 4 product confirming the mechanism predicted by the homology model. Moreover, a Saturation Transfer
 5 Difference (STD) experiment was used to probe UDP- α -D-glucose binding to UGT74B1. In this
 6 experiment, the signals of the UDP- α -D-glucose atoms are modulated in intensity depending on how closely
 7 they bind to UGT74B1 (Fig. 2). The relative ranking of this modulation shows that UDP- α -D-glucose is
 8 strongly bound to UGT74B1 by its aromatic base and less by its glucosyl moiety. This result is in full
 9 agreement with binding modes predicted through molecular docking where the aromatic ring is stabilized
 10 by a strong and close range π -stacking interaction [25].

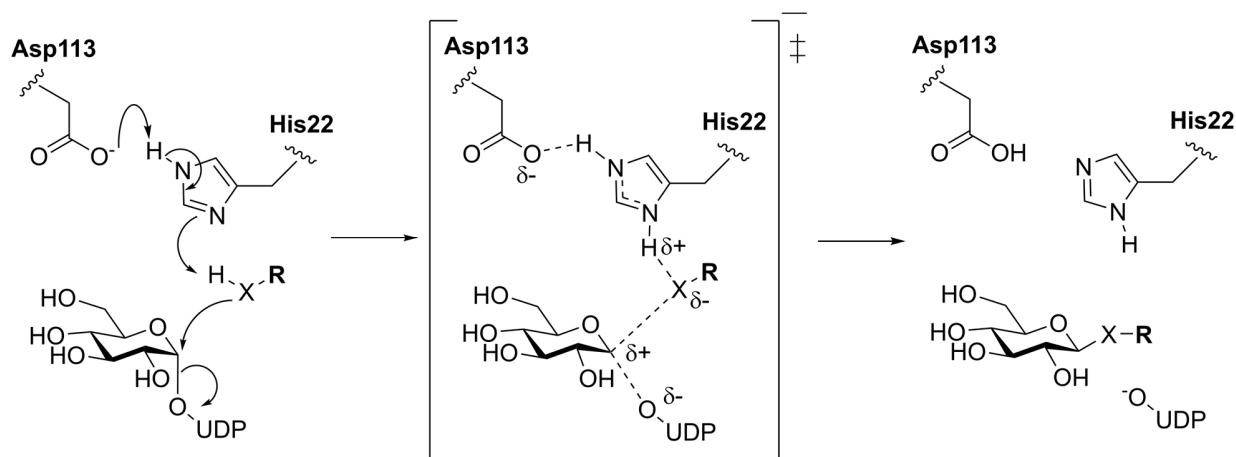
11



12
 13 **Figure 2:** (A) 1D ¹H NMR spectrum of the mixture of UGT74B1 and UDP- α -D-glucose and (B) the
 14 corresponding STD-NMR (600MHz, T=298K, phosphate buffer pH 7.3). (C) Epitope mapping of UDP- α -
 15 D-glucose.

16
 17 Like most GT1 reported structures, UGT74B1 exhibits a catalytic dyad formed of a carboxylic acid
 18 amino acid (Asp113) in close contact with an histidine (His22), which is located in the suitable distance to
 19 deprotonate the acceptor (Fig. 3). It has to be noted that hydroximates and thiohydroximates can exist under
 20 two tautomeric forms (Fig 1.B). Yet, deprotonation of both tautomers will eventually lead to the nucleophilic
 21 attack of either oxygen or sulfur, depending on the substrate considered. This mechanism is similar to the
 22 triad observed in a serine protease mechanism. Both residues were also identified as the potential catalytic
 23 dyad in the homology model built by Kopycki *et al.* [31]. However the role of these residues is still unclear
 24 as some GT1 do not possess these two amino acids [37] and several studies have demonstrated that unlike

1 *O*-glycosylation, the histidine residue was not involved catalytically in *N*-glycosylation reactions [16,38].
 2 In contrast to hydroxyl that needs to be deprotonated to avoid the formation of a highly unstable positively
 3 charged oxonium ion (R1-OH⁺-R2), amines can readily form a positively charged intermediate without
 4 preliminary deprotonation [16]. In order to elucidate the role of these two residues in the catalytic
 5 mechanism of UGT74B1, we have generated two mutants in which either His22 or Asp113 were replaced
 6 with the non-reactive alanine.
 7



8
 9 **Figure 3:** Proposed SN₂ mechanism of glycosylation reaction catalyzed by UGT74B1 (X=O or S). *Asp113*
 10 and *His22* are depicted as putative components of the catalytic dyad, as identified with the homology model
 11 of UGT74B1.

12
 13 Both mutants were expressed and purified. However Asp113Ala could not be purified to homogeneity
 14 on Immobilized Metal-Affinity Chromatography column, unlike His22Ala that could be purified in quantity
 15 as high as WT UGT74B1 (typically 10 mg. l⁻¹ culture) (Fig. S8-A). His22Ala mutation abolished enzymatic
 16 activity, as no activity could be detected in our assay (Fig. S8-B). This indicates that this residue is critical
 17 to deprotonate thiol acceptors before the nucleophilic attack (like in other GT1 *O*-glycosylation mechanism).

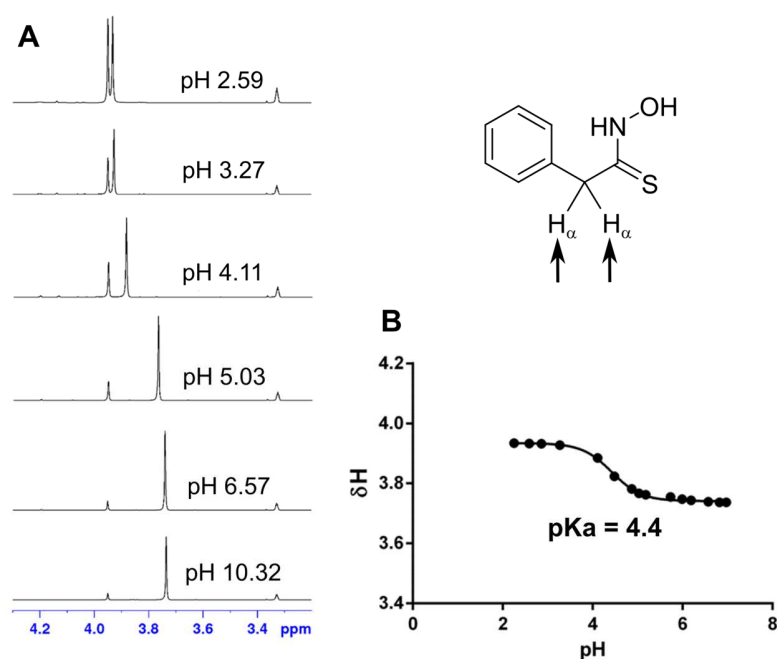
18 Unlike His22, the contribution of Asp113 in promoting this deprotonation is unclear as Asp113Ala
 19 mutant still exhibited enzymatic activity. The Michaelis Menten fit of PATH or PPTH concentration
 20 dependence (Fig. S8-B) gave respective Michaelis constants K_M of 27 μ M and 59 μ M, higher than the value
 21 calculated for WT UGT74B1 (Table 1). However, the catalytic turnover k_{cat} could not be determined, as
 22 Asp113Ala mutant could not be obtained as a pure enzyme. Maximum velocity V_{max} was determined to be
 23 1.2 and 2.4 μ M.min⁻¹ for each substrate, indicating that Asp113Ala residual activity is not insignificant,
 24 considering the low amount of impure enzyme introduced in the reaction mixture.

25 These mutation studies indicated that the acceptor acidity is crucial in UGT74B1 activity, and to assess
 26 this hypothesis we determined the pKa of sulfur- (PATH, PPTH) and oxygen- (PAH, PPH) containing

1 acceptors. Concerning pKa values, no recent data were available for thiohydroximates in the literature [39].
2 Acidity constants of all four substrates were thus determined by NMR.

3 Protons located on the alpha-carbon (H_{α}) of the 4 substrates were used as probes for pKa determination
4 (Fig. 4-A). Chemical shifts of both protons were determined in a range of buffered solutions, and plotting
5 of $\delta=f(\text{pH})$ gave a sigmoidal curve fitting, which inflexion point corresponding to experimental pKa (Fig.
6 4-B). This methodology was successfully used for other acidity constant determinations [40,41]

7
8 The calculated values for all 4 substrates were PATH: 4.4; PPTH: 4.6; PAH: 9.2; PPH: 9.4. (See Fig.
9 S9 to S11) The values for thiohydroximates, are close to those (between 4.0 and 5.6) reported by Nagata *et*
10 *al.* [39].



11
12
13 **Figure 4:** PATH pKa determination by NMR. (A) ¹H NMR spectrum of PATH. Arrow indicates
14 protons and corresponding signals used for pKa determination. (B) Evolution of chemical shift with pH
15 and pKa determination.

16
17 **3.3 GT activity is correlated to the pKa of the nucleophile acceptor**
18 pKa comparison of thiohydroximates and hydroximates indicates that a low pKa (PATH and PPTH)
19 gives a higher enzymatic activity than a high pKa (PAH and PPH). This can be understood as
20 thiohydroximates can easily form the corresponding thiolates after His22 deprotonation, and thus are more
21 reactive than their hydroximate counterparts. However, because the pKa values do not cover a wide range

1 of values (pKa values gap between 5 and 9), the correlation between pKa and enzymatic activity is not
2 obvious.

3 To evaluate this potential correlation, we have used simple acceptors, that cover a more extended pKa
4 range (Fig. 1 and Table 2). The selected compounds were *O*-containing chloro-substituted phenols (4-
5 chlorophenol CP, 2,3- 2,4- and 2,5 dichlorophenols DCP, 2,3,4- 2,4,5- 2,4,6- trichlorophenols TCP) and *S*-
6 containing thiophenols (4-chlorothiophenol CTP and thiophenol TP), presenting a calculated pKa range
7 between 5.5 and 9.0. To validate the *in silico* calculation of pKa, pKa determination by NMR was applied
8 to CTP (Fig. S12), giving a value similar to the calculated value (respectively 5.8 and 5.5).

9

Acceptor	pKa ^a	K _M (μM)	k _{cat} (min ⁻¹)	k _{cat} /K _M (min ⁻¹ .mM ⁻¹)
PATH	4.4 ^a	3.1 ± 0.6	280 ± 58	90 x 10 ³
PPTH	4.6 ^a	2.2 ± 0.5	326 ± 95	148 x 10 ³
PAH	9.2 ^a	1.1 ± 0.2	3.9 ± 1.3	3.5 x 10 ³
PPH	9.4 ^a	0.9 ± 0.2	4.3 ± 1.2	4.8 x 10 ³
4-CTP	5.8 ^a /5.5 ^b	215 ± 13	139.0 ± 5.6	647
TP	6.6 ^b	105 ± 24	10.9 ± 1.5	104
2,4,6-TCP	6.0 ^b	132 ± 24	14.5 ± 1.3	110
2,4,5-TCP	6.8 ^b	130 ± 45	6.1 ± 1.1	47
2,3,4-TCP	7.0 ^b	147 ± 6	6.6 ± 0.9	45
2,5-DCP	7.2 ^b	132 ± 23	4.2 ± 0.2	32
2,3-DCP	7.4 ^b	195 ± 26	1.9 ± 0.3	10
2,4-DCP	7.4 ^b	148 ± 5	2.2 ± 0.3	15
4-CP	9.0 ^b	149 ± 43	0.6 ± 0.2	3

10 **Table 2:** Catalytic constants and pKa of thiohydroxamic acids, hydroxamic acids, phenol and thiophenol
11 derivatives. Values were obtained at 37°C, pH 8.0. ^ameasured by NMR; ^b calculated using ACD/Labs.

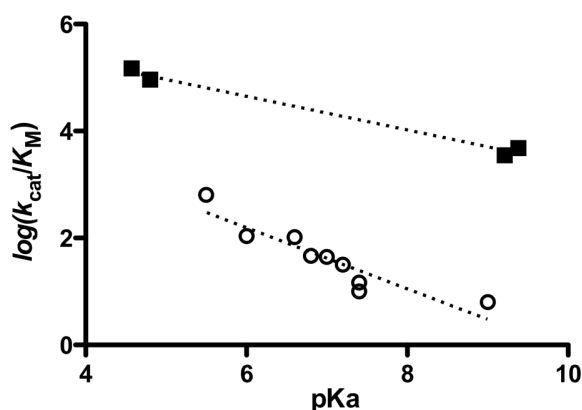
12 *CTP: Chlorothiophenol; TP: Thiophenol; TCP: Trichlorophenol; DCP: Dichlorophenol; CP:*
13 *Chlorophenol.*

14 Because of their lower solubility, phenols can interfere with the tri-enzymatic assay used that couples
15 UDP formation by UGT74B1 with NADH consumption. The latter is determined spectrophotometrically at
16 340 nm. We have set up an activity assay based on HPLC separation of phenols and the corresponding
17 glycosylated products. When validated by using PATH and PPTH as substrates, this assay gave similar
18 catalytic constants as those presented in Table 1 (data not shown).

19 All eight phenols and thiophenols were used as acceptors in UGT74B1 reaction, and their catalytic
20 constants were determined (Table 2). All compounds are glycosylated by UGT74B1 when using UDP-α-

1 glucose as sugar donor. They all exhibit similar K_M values (100-200 μM), higher than those determined for
2 hydroximates or thiohydroximates, probably because phenols might establish less stabilizing interactions in
3 UGT74B1 active site. The observed rates fit those reported by Braziers-Hicks *et al.*, as 2,4,5-TCP is one
4 order of magnitude less active than 4-CTP [16].

5 The resulting Brønsted analysis of glycosylation provides evidence of a correlation between enzymatic
6 efficiency k_{cat}/K_M and pKa of the acceptor (Fig. 5). Unlike other studies on nucleophile pKa dependence of
7 GT activity [42], the corresponding slope calculated $\beta_{\text{nu}}=-0.64$ ($R^2=0.91$) for UGT74B1 is negative. As β_{nu}
8 value can give an estimate of the change in effective charge on the nucleophile towards the transition state
9 [43], acceptor nucleophilic atoms (*O*- or *S*-) in UGT74B1 have a negative charge accumulation during
10 catalysis, which is in agreement with the transient formation of deprotonated thiolate or hydroxylate during
11 catalysis (Fig. 3)



12
13 **Figure 5:** Brønsted plot of k_{cat}/K_M for all tested UGT74B1 substrates. Values for thiohydroxamic and
14 hydroxamic acids are depicted as black squares. Data corresponding to thiophenol and phenol derivatives
15 are marked as white circles.

16
17 A similar enzymatic mechanism can be proposed for thiohydroximates and hydroximates, although no
18 data is available between pKa values of 5 and 9. Brønsted analysis gives also a negative slope $\beta_{\text{nu}}=-0.31$,
19 although shallower than for phenols. During catalysis, thiohydroximates and hydroximates accumulate less
20 negative charge on nucleophilic atoms, and are more sensitive to general acid/base mechanism than phenols.

21 In both cases, the Brønsted analyses do not demonstrate that the nature of the nucleophilic atom is
22 critical for catalysis, as there is a continuum in linear correlation – especially for phenolic derivatives.

23 4. Discussion

24 In *Brassicaceae* plants, UGT74B1 was originally identified as a key enzyme in the biosynthesis of
25 glucosinolates, catalyzing the *S*-glucosylation of thiohydroximates [30,44]. The enzyme was annotated as a
26 *S*-glycosyltransferase in genomic data, like other GTs where the specificity of atom that form the glycosidic

1 bond is highlighted [35]. However many GTs have been reported to be able to use acceptors containing
2 diverse nucleophilic atoms, which calls into question the canonic specificity of GTs towards one particular
3 atom [15–22,24].

4 Nevertheless, the corresponding studies did not dissected in detail the molecular mechanism underlying
5 this broader specificity. More precisely, the influence of nucleophile's nature on enzyme reactivity was not
6 examined into detail.

7 UGT74B1 was shown to glycosylate *S*- and *O*-containing acceptors, such as hydroximates, the structure
8 of which is closely related to the natural acceptor thiohydroximates. The ratio of catalytic efficiency between
9 both families of analogues is of 2 orders of magnitude (10^5 and 10^3 min⁻¹.mM⁻¹ range respectively for
10 thiohydroximates and hydroximates). This catalytic efficiency towards *O*-acceptors is not negligible, as
11 other GT1 enzymes exhibited similar kinetic constants towards their “natural” substrates [16,45]. Thus,
12 UGT74B1 can efficiently catalyze *O*- and *S*-glycosylation *in vitro* when using appropriate acceptors, but is
13 solely catalyzing the latter *in vivo* because only endogenous thiohydroximates are efficiently binding to the
14 enzyme and exhibit low pKa.

15 To assess this versatility of UGT74B1 towards *O*- and *S*-acceptors, a range of chloro-substituted
16 thiophenols and phenols were also used as substrates by UGT74B1. More interestingly, when plotting the
17 logarithm of the second order rate k_{cat}/K_M vs. pKa values of (thio)phenols, a linear correlation could be fitted,
18 and Brønsted-type relationship was demonstrated, with a negative β_{nu} value (Fig. 5). The acceptor
19 nucleophilic atom shows a decrease in effective charge during the catalysis towards the transition state. A
20 transition state where the proton abstraction by His22 is significantly advanced, whereas the glycosidic bond
21 formation is not, can explain this negative β_{nu} value. As a lower absolute value for β_{nu} value can be estimated
22 in the case of hydroximates and thiohydroximates, these substrates are less prone to general base catalysis
23 by His22 [43,46].

24 UGT74B1 is not the first example of a GT able to generate several glycosidic linkages, when
25 considering the nature of the atom involved in the bond. However, the Brønsted-type relationship for
26 (thio)phenol glycosylation does not exhibit a break between *O*- and *S*- acceptors. The influence of pKa on
27 the reactivity overtakes the nature of the nucleophilic atom. UGT74B1 reactivity is therefore mostly driven
28 by the predisposition of the nucleophile chemical property to be energetically close to the transition state,
29 and thus decreasing the activation energy. The enzyme can accommodate and use several nucleophiles as
30 acceptors, as long as they satisfy the chemistry underlying the catalysis.

31 The dissected mechanism of UGT74B1 can be used as a paradigm for other GTs able to use several
32 acceptors of similar shape, size, and properties, bearing different nucleophilic atoms, and redefine the
33 conventional nomenclature that classifies a GT according to the nature of the nucleophilic atom.

Acknowledgments & funding sources

The authors thank G. Jousset and A. Duvergé for technical help in producing and characterizing UGT74B1 wild-type and mutants' activities. PL, RD, MS, AT, SMar, GC and HO thank the Labex SynOrg (ANR-11-LABX-0029) for financial support. SMar, GC and HO thank the Région Normandie, CNRS, the University and INSA of Rouen for financial support. SMarq and SMarr were funded by French Ministry of Research.

Declaration of interest

The authors declares that there is no conflict of interest.

References

- [1] L.L. Lairson, B. Henrissat, G.J. Davies, S.G. Withers, Glycosyltransferases: Structures, Functions, and Mechanisms, *Annu. Rev. Biochem.* 77 (2008) 521–555.
doi:10.1146/annurev.biochem.76.061005.092322.
- [2] K. Xie, R. Chen, J. Li, R. Wang, D. Chen, X. Dou, J. Dai, Exploring the Catalytic Promiscuity of a New Glycosyltransferase from *Carthamus tinctorius*, *Org. Lett.* 16 (2014) 4874–4877.
doi:10.1021/ol502380p.
- [3] A. Ardèvol, C. Rovira, Reaction Mechanisms in Carbohydrate-Active Enzymes: Glycoside Hydrolases and Glycosyltransferases. Insights from ab Initio Quantum Mechanics/Molecular Mechanics Dynamic Simulations, *J. Am. Chem. Soc.* 137 (2015) 7528–7547.
doi:10.1021/jacs.5b01156.
- [4] A. Varki, Biological roles of oligosaccharides: all of the theories are correct, *Glycobiology.* 3 (1993) 97–130. doi:10.1093/glycob/3.2.97.
- [5] R.G. Spiro, Protein glycosylation: nature, distribution, enzymatic formation, and disease implications of glycopeptide bonds, *Glycobiology.* 12 (2002) 43R–56R.
doi:10.1093/glycob/12.4.43R.
- [6] P. Lafite, R. Daniellou, Rare and unusual glycosylation of peptides and proteins., *Nat. Prod. Rep.* 29 (2012) 729–38. doi:10.1039/c2np20030a.
- [7] R.T. Dere, A. Kumar, V. Kumar, X.M. Zhu, R.R. Schmidt, Synthesis of Glycosylthiols and Reactivity Studies, *J Org Chem.* 76 (2011) 7539–7545. doi:10.1021/jo200624e.
- [8] J.D.C. Codee, R.E.J.N. Litjens, L.J. van den Bos, H.S. Overkleeft, G.A. van der Marel, Thioglycosides in sequential glycosylation strategies, *Chem. Soc. Rev.* 34 (2005) 769–782.
doi:10.1039/B417138C.
- [9] H. Driguez, Thiooligosaccharides as Tools for Structural Biology, *ChemBiochem.* 2 (2001) 311–

- 1 318. doi:10.1002/1439-7633(20010504)2:5<311::AID-CBIC311>3.0.CO;2-L.
- 2 [10] M. Brito-Arias, C-Glycosides, in: Synth. Charact. Glycosides, Springer US, Boston, MA, 2007: pp.
- 3 247–271. doi:10.1007/978-0-387-70792-1_5.
- 4 [11] A. Chang, S. Singh, G.N. Phillips Jr, J.S. Thorson, Glycosyltransferase structural biology and its
- 5 role in the design of catalysts for glycosylation, *Curr. Opin. Biotech.* 22 (2011) 800–808.
- 6 doi:http://dx.doi.org/10.1016/j.copbio.2011.04.013.
- 7 [12] M.M. Palcic, Glycosyltransferases as biocatalysts, *Curr. Opin. Chem. Biol.* 15 (2011) 226–233.
- 8 doi:10.1016/j.cbpa.2010.11.022.
- 9 [13] S.M. Hancock, M.D. Vaughan, S.G. Withers, Engineering of glycosidases and
- 10 glycosyltransferases, *Curr. Opin. Chem. Biol.* 10 (2006) 509–519. doi:10.1016/j.cbpa.2006.07.015.
- 11 [14] J. Ati, P. Lafite, R. Daniellou, Enzymatic synthesis of glycosides: from natural O- and N-
- 12 glycosides to rare C- and S-glycosides, *Beilstein J. Org. Chem.* 13 (2017) 1857–1865.
- 13 doi:10.3762/bjoc.13.180.
- 14 [15] C. Wen, W. Huang, X.-L. Zhu, X.-S. Li, F. Zhang, R.-W. Jiang, UGT74AN1, a Permissive
- 15 Glycosyltransferase from *Asclepias curassavica* for the Regiospecific Steroid 3- O -Glycosylation,
- 16 *Org. Lett.* 20 (2018) 534–537. doi:10.1021/acs.orglett.7b03619.
- 17 [16] M. Brazier-Hicks, W.A. Offen, M.C. Gershater, T.J. Revett, E.-K. Lim, D.J. Bowles, G.J. Davies,
- 18 R. Edwards, Characterization and engineering of the bifunctional N- and O-glucosyltransferase
- 19 involved in xenobiotic metabolism in plants, *Proc. Natl. Acad. Sci. U. S. A.* 104 (2007) 20238–
- 20 20243. doi:10.1073/pnas.0706421104.
- 21 [17] R.W. Gantt, R.D. Goff, G.J. Williams, J.S. Thorson, Probing the Aglycon Promiscuity of an
- 22 Engineered Glycosyltransferase, *Angew. Chem. Int. Ed.* 47 (2008) 8889–8892.
- 23 doi:10.1002/anie.200803508.
- 24 [18] M.L. Falcone Ferreyra, E. Rodriguez, M.I. Casas, G. Labadie, E. Grotewold, P. Casati,
- 25 Identification of a bifunctional maize C- and O-glucosyltransferase, *J. Biol. Chem.* 288 (2013)
- 26 31678–31688. doi:10.1074/jbc.M113.510040.
- 27 [19] Y. Wang, W.-J. Wang, C. Su, D.-M. Zhang, L.-P. Xu, R.-R. He, L. Wang, J. Zhang, X.-Q. Zhang,
- 28 W.-C. Ye, Cytotoxic quassinoids from *Ailanthus altissima*, *Bioorg Med Chem Lett.* 23 (2013)
- 29 654–657. doi:10.1016/j.bmcl.2012.11.116.
- 30 [20] H. Wang, T.J. Oman, R. Zhang, C. V Garcia De Gonzalo, Q. Zhang, W.A. van der Donk, The
- 31 glycosyltransferase involved in thurandacin biosynthesis catalyzes both O- and S-glycosylation, *J.*
- 32 *Am. Chem. Soc.* 136 (2014) 84–87. doi:10.1021/ja411159k.
- 33 [21] D. Chen, R. Chen, R. Wang, J. Li, K. Xie, C. Bian, L. Sun, X. Zhang, J. Liu, L. Yang, F. Ye, X.
- 34 Yu, J. Dai, Probing the Catalytic Promiscuity of a Regio- and Stereospecific C-Glycosyltransferase
- 35 from *Mangifera indica*, *Angew. Chemie.* 127 (2015) 12869–12873. doi:10.1002/ange.201506505.

- 1 [22] F. Gandia-Herrero, A. Lorenz, T. Larson, I.A. Graham, D.J. Bowles, E.L. Rylott, N.C. Bruce,
2 Detoxification of the explosive 2,4,6-trinitrotoluene in Arabidopsis: discovery of bifunctional O-
3 and C-glucosyltransferases, *Plant J.* 56 (2008) 963–974.
- 4 [23] A. Gutmann, B. Nidetzky, Enzymatic C-glycosylation: Insights from the study of a complementary
5 pair of plant O- and C-glucosyltransferases, *Pure Appl. Chem.* 85 (2013) 1865–1877.
6 doi:10.1351/pac-con-12-11-24.
- 7 [24] A. Gutmann, B. Nidetzky, Switching between O- and C-Glycosyltransferase through Exchange of
8 Active-Site Motifs, *Angew Chem Int Ed.* 51 (2012) 12879–12883. doi:10.1002/anie.201206141.
- 9 [25] S. Marroun, S. Montaut, S. Marquès, P. Lafite, G. Coadou, P. Rollin, G. Jousset, M. Schuler, A.
10 Tatibouët, H. Oulyadi, R. Daniellou, UGT74B1 from Arabidopsis thaliana as a versatile biocatalyst
11 for the synthesis of desulfoglycosinolates, *Org. Biomol. Chem.* 14 (2016) 6252–6261.
12 doi:10.1039/c6ob01003b.
- 13 [26] J. Stepper, S. Shastri, T.S. Loo, J.C. Preston, P. Novak, P. Man, C.H. Moore, V. Havlicek, M.L.
14 Patchett, G.E. Norris, Cysteine S-glycosylation, a new post-translational modification found in
15 glycopeptide bacteriocins, *FEBS Lett.* 585 (2011) 645–650. doi:10.1016/j.febslet.2011.01.023.
- 16 [27] T.J. Oman, J.M. Boettcher, H. Wang, X.N. Okalibe, W.A. van der Donk, Sublancin is not a
17 lantibiotic but an S-linked glycopeptide, *Nat. Chem. Biol.* 7 (2011) 78–80.
18 doi:10.1038/nchembio.509.
- 19 [28] H. Wang, W.A. van der Donk, Substrate selectivity of the sublancin S-glycosyltransferase, *J Am*
20 *Chem Soc.* 133 (2011) 16394–16397. doi:10.1021/ja2075168.
- 21 [29] Y.S.Y. Hsieh, B.L. Wilkinson, M.R. O’Connell, J.P. Mackay, J.M. Matthews, R.J. Payne,
22 Synthesis of the Bacteriocin Glycopeptide Sublancin 168 and S-Glycosylated Variants, *Org Lett.*
23 14 (2012) 1910–1913. doi:10.1021/ol300557g.
- 24 [30] C.D. Grubb, B.J. Zipp, J. Ludwig-Müller, M.N. Masuno, T.F. Molinski, S. Abel, Arabidopsis
25 glucosyltransferase UGT74B1 functions in glucosinolate biosynthesis and auxin homeostasis.,
26 *Plant J.* 40 (2004) 893–908. doi:10.1111/j.1365-313X.2004.02261.x.
- 27 [31] J. Kopycki, E. Wieduwild, J. Kohlschmidt, W. Brandt, A.N. Stepanova, J.M. Alonso, M.S. Pedras,
28 S. Abel, C.D. Grubb, Kinetic analysis of Arabidopsis glucosyltransferase UGT74B1 illustrates a
29 general mechanism by which enzymes can escape product inhibition, *Biochem. J.* 450 (2013) 37–
30 46. doi:10.1042/bj20121403.
- 31 [32] S. Yoganathan, S.J. Miller, N-Methylimidazole-catalyzed Synthesis of Carbamates from
32 Hydroxamic Acids via the Lossen Rearrangement, *Org. Lett.* 15 (2013) 602–605.
33 doi:10.1021/ol303424b.
- 34 [33] N. Ohtsuka, M. Okuno, Y. Hoshino, K. Honda, A base-mediated self-propagative Lossen
35 rearrangement of hydroxamic acids for the efficient and facile synthesis of aromatic and aliphatic

- 1 primary amines, *Org. Biomol. Chem.* 14 (2016) 9046–9054. doi:10.1039/C6OB01178K.
- 2 [34] M. Jia, H. Zhang, Y. Lin, D. Chen, Y. Chen, Y. Xia, Consecutive Lossen
3 rearrangement/transamidation reaction of hydroxamic acids under catalyst- and additive-free
4 conditions, *Org. Biomol. Chem.* 16 (2018) 3615–3624. doi:10.1039/C8OB00490K.
- 5 [35] V. Lombard, H. Golaconda Ramulu, E. Drula, P.M. Coutinho, B. Henrissat, The carbohydrate-
6 active enzymes database (CAZy) in 2013, *Nucleic Acids Res.* 42 (2014) D490-5.
7 doi:10.1093/nar/gkt1178.
- 8 [36] N. Ibrahim, I. Allart-Simon, G.R. De Nicola, R. Iori, J.-H. Renault, P. Rollin, J.-M. Nuzillard,
9 Advanced NMR-Based Structural Investigation of Glucosinolates and Desulfoglucosinolates, *J.*
10 *Nat. Prod.* 81 (2018) 323–334. doi:10.1021/acs.jnatprod.7b00776.
- 11 [37] D. Dong, R. Ako, M. Hu, B. Wu, Understanding substrate selectivity of human UDP-
12 glucuronosyltransferases through QSAR modeling and analysis of homologous enzymes.,
13 *Xenobiotica.* 42 (2012) 808–20. doi:10.3109/00498254.2012.663515.
- 14 [38] A.-S. Patana, M. Kurkela, M. Finel, A. Goldman, Mutation analysis in UGT1A9 suggests a
15 relationship between substrate and catalytic residues in UDP-glucuronosyltransferases., *Protein*
16 *Eng. Des. Sel.* 21 (2008) 537–43. doi:10.1093/protein/gzn030.
- 17 [39] K. Nagata, S. Mizukami, Studies on Thiohydroxamic Acids and Their Metal Chelates. II.
18 Structures of Thiohydroxamic Acids, *Chem. Pharm. Bull. (Tokyo).* 14 (1966) 1255–1262.
19 doi:10.1248/cpb.14.1255.
- 20 [40] J. Bezençon, M.B. Wittwer, B. Cutting, M. Smieško, B. Wagner, M. Kansy, B. Ernst, pKa
21 determination by ¹H NMR spectroscopy – An old methodology revisited, *J. Pharm. Biomed. Anal.*
22 93 (2014) 147–155. doi:10.1016/j.jpba.2013.12.014.
- 23 [41] K. Popov, H. Rönkkömäki, L.H.J. Lajunen, Guidelines for NMR measurements for determination
24 of high and low pKa values (IUPAC Technical Report), *Pure Appl. Chem.* 78 (2006) 663–675.
25 doi:10.1351/pac200678030663.
- 26 [42] S.S. Lee, S.Y. Hong, J.C. Errey, A. Izumi, G.J. Davies, B.G. Davis, Mechanistic evidence for a
27 front-side, S_Ni-type reaction in a retaining glycosyltransferase, *Nat Chem Biol.* 7 (2011) 631–638.
28 doi:10.1038/nchembio.628.
- 29 [43] J.-D. Ye, N.-S. Li, Q. Dai, J.A. Piccirilli, The Mechanism of RNA Strand Scission: An
30 Experimental Measure of the Brønsted Coefficient, β_{nuc} , *Angew. Chemie Int. Ed.* 46 (2007) 3714–
31 3717. doi:10.1002/anie.200605124.
- 32 [44] B.A. Halkier, J. Gershenzon, Biology and biochemistry of glucosinolates, *Annu. Rev. Plant Biol.*
33 57 (2006) 303–333.
- 34 [45] X. Wang, Structure, mechanism and engineering of plant natural product glycosyltransferases,
35 *FEBS Lett.* 583 (2009) 3303–3309. doi:10.1016/j.febslet.2009.09.042.

1 [46] M.S. Macauley, K.A. Stubbs, D.J. Vocadlo, O-GlcNAcase catalyzes cleavage of thioglycosides
2 without general acid catalysis, *J. Am. Chem. Soc.* 127 (2005) 17202–17203.
3 doi:10.1021/ja0567687.
4
5